arXiv:hep-ph/0408138v1 11 Aug 2004

TU-726
hep-ph/0408138

Measurement of Squark Flavor Mixings in Supersymmetric Models at Super B Factory

Motoi Endo[1] and **Satoshi Mishima**[2]

Department of Physics, Tohoku University, Sendai 980-8578, Japan

Abstract

We discuss potential to measure squark flavor mixings based on future data at super B factory and LHC. In particular we focus on the imaginary part of the mixings by investigating the CP violating observables. As a result, we find they are determined with the uncertainty about 10 % at best.

[1]E-mail: endo@tuhep.phys.tohoku.ac.jp
[2]E-mail: mishima@tuhep.phys.tohoku.ac.jp

The naturalness problem inherent in the standard model (SM) implies new physics beyond the SM at the electroweak scale. Low scale supersymmetry is one of the most promising solutions to the problem. We expect to detect and measure such a new physics at TeV scale by high energy collider experiment at LHC in the near future. In the case of supersymmetry models, LHC might discover some colored supersymmetric particles and establish the presence of supersymmetry or its extension. In such an era, we shall proceed to the next step, the determination of model parameters. This is inevitable for further study of physics at high energy scale, including flavor structure and its origin.

The flavor-changing-neutral-current (FCNC) is one of the most attractive phenomena to investigate supersymmetry and further physics at higher energy scale. In fact FCNC in the SM is sufficiently suppressed by the GIM mechanism. In contrast, the minimal supersymmetric standard model (MSSM) has the additional particles, and the superpartner of matters has flavor mixings in the mass matrix. FCNC is then sensitive to these mixings and becomes large generically. The flavor mixings between first two generations are strongly constrained from the $K^0 - \overline{K}^0$ mixing, and $1-3$ mixings are also limited experimentally. On the other hand, the supersymmetry contributions to squark flavor changing amplitudes between $2-3$ generations, in which we study especially the $b \to s$ transition here, may be large even when we consider the experimental constraint from the inclusive branching ratio of $b \to s\gamma$ and the neutron and atomic EDMs [1–3]. That is, the $b \to s$ transition is useful to study models of supersymmetry.

The squark mixings generally have an $\mathcal{O}(1)$ phase and induce CP violation. Furthermore as noted later, the processes which have both violations of CP and flavor are much sensitive to the imaginary part of the squark mixings. Thus we expect it to be possible to measure those parameters without suffering from large uncertainties in future experiments.

In addition, one of the most attractive processes which include both CP violating and flavor changing is the mixing-induced CP asymmetry for $B_d \to \phi K_S$. Belle has reported large deviation, $S_{\phi K_S} = -0.96 \pm 0.50^{+0.09}_{-0.11}$ [4], from the SM prediction, which is 3.5σ away, though BABAR result is $S_{\phi K_S} = 0.47 \pm 0.34^{+0.08}_{-0.06}$ [5] in agreement with the SM. Indeed the situation is not settled yet, however if the Belle result is correct, it is not only the first signal for new physics through $b \to s$ FCNC processes, but also it implies large CP violating phase in the scalar bottom to strange flavor mixings [1,6–8]. Therefore in this letter we focus on the situation that CP symmetry is almost maximally violated in the $b \to s$ squark mixings.

Although the masses of the supersymmetric particles will be measured at LHC, in order to study the flavor mixings in the squark mass matrices we need some experiments with high luminosity. Particularly super B factory with the luminosity of $10^{35}\,\mathrm{cm}^{-2}\mathrm{sec}^{-1}$ is very useful for the measurement of the $b \to s$ mixings. Actually various FCNC processes with CP violation are proposed to be measured with high accuracy. In this letter we focus on the CP violating

processes, the mixing-induced CP asymmetry of $B_d \to \phi K_S$ ($S_{\phi K_S}$), of $B_d \to \eta' K_S$ ($S_{\eta' K_S}$), of $B_d \to K^* \gamma$ ($S_{K^*\gamma}$), the direct CP asymmetry of $b \to s\gamma$ ($A_{\rm CP}^{b\to s\gamma}$) and the $B_s - \overline{B_s}$ mixing (ΔM_s), after one year of running at super B factory.

So far many studies for the supersymmetric contributions to the $b \to s$ transitions have been made. Some are interested in potential to detect the MSSM and some flavor models through the transition processes. The authors in Ref. [9] investigated the processes in systematic way for some typical flavor models in supersymmetry. Their study is not only to search potential for detection but also to identify these models at super B factory and they showed that the processes are very helpful. However this argument is based on model dependent analysis. Rather for the purpose of investigation of higher scale physics more definitely, we need model independent one. Therefore in this letter we do not assume any flavor models, and study the $b \to s$ transition processes in model independent way.

The mass insertion approximation (MIA) [10, 11] is a powerful technique for model independent analysis of the MSSM. When off-diagonal elements in the squark mass matrices are small enough, the squark propagators with $\tilde{b} \to \tilde{s}$ FCNC can be expanded as a series in terms of

$$
\begin{aligned}
(\delta^d_{LL})_{23} &= \frac{(m^2_{\tilde{d}_L})_{23}}{m^2_{\tilde{q}}} \ , \qquad & (\delta^d_{RR})_{23} &= \frac{(m^2_{\tilde{d}_R})_{23}}{m^2_{\tilde{q}}} \ , \\
(\delta^d_{LR})_{23} &= \frac{(m^2_{\tilde{d}_{LR}})_{23}}{m^2_{\tilde{q}}} \ , \qquad & (\delta^d_{RL})_{23} &= (\delta^d_{LR})^*_{32} \ ,
\end{aligned}
\tag{1}
$$

where $m^2_{\tilde{d}}$ is the squared down-type-squark mass matrix, $m_{\tilde{q}}$ an averaged squark mass. There is chirality structure in the squark mass matrices. It is important that these parameters generically have an $\mathcal{O}(1)$ phase and imaginary part of them induces CP and flavor violations simultaneously. In this letter we discuss potential to constrain and measure these MIA parameters by the data of the $b \to s$ transition processes which will be measured in future at super B factory and LHC.

Here we summarize the effective Hamiltonian for $\Delta B = 1$ and $\Delta S = 1$ processes [12]. This is defined as

$$
H_{\rm eff} \ = \ \frac{4G_F}{\sqrt{2}} \left[\sum_{q'=u,c} V_{q'b} V^*_{q's} \sum_{i=1,2} C_i O_i^{(q')} - V_{tb} V^*_{ts} \sum_{i=3\sim 6,7\gamma,8G} \left(C_i O_i + \widetilde{C}_i \widetilde{O}_i \right) \right] \ , \tag{2}
$$

where the local operators are given by

$$
\begin{aligned}
O_1^{(q')} &= (\bar{s}_i \gamma_\mu P_L q'_j)(\bar{q}'_j \gamma^\mu P_L b_i) \ , \qquad & O_2^{(q')} &= (\bar{s}_i \gamma_\mu P_L q'_i)(\bar{q}'_j \gamma^\mu P_L b_j) \ , \\
O_3 &= (\bar{s}_i \gamma_\mu P_L b_i) \sum_q (\bar{q}_j \gamma^\mu P_L q_j) \ , \qquad & O_4 &= (\bar{s}_i \gamma_\mu P_L b_j) \sum_q (\bar{q}_j \gamma^\mu P_L q_i) \ , \\
O_5 &= (\bar{s}_i \gamma_\mu P_L b_i) \sum_q (\bar{q}_j \gamma^\mu P_R q_j) \ , \qquad & O_6 &= (\bar{s}_i \gamma_\mu P_L b_j) \sum_q (\bar{q}_j \gamma^\mu P_R q_i) \ ,
\end{aligned}
$$

$$O_{7\gamma} = \frac{e}{16\pi^2} m_b \bar{s}_i \sigma^{\mu\nu} P_R b_i F_{\mu\nu} \ , \qquad O_{8G} = \frac{g_s}{16\pi^2} m_b \bar{s}_i \sigma^{\mu\nu} P_R T^a_{ij} b_j G^a_{\mu\nu} \ , \tag{3}$$

with $P_R = (1+\gamma_5)/2$ and $P_L = (1-\gamma_5)/2$. Here, i and j are color indices, and q is taken to be u, d, s and c. The terms with tilde are obtained by flipping chiralities, $L \leftrightarrow R$, in Eq. (3). The gluino contributions to the Wilson coefficients C_i at supersymmetry scale M_S are calculated as

$$\begin{aligned}
C_3^{\tilde{g}}(M_S) &\simeq \frac{\sqrt{2}\alpha_s^2}{4G_F V_{tb}V_{ts}^* m_{\tilde{q}}^2}(\delta^d_{LL})_{23}\left[-\frac{1}{9}B_1(x) - \frac{5}{9}B_2(x) - \frac{1}{18}P_1(x) - \frac{1}{2}P_2(x)\right] \ , \\
C_4^{\tilde{g}}(M_S) &\simeq \frac{\sqrt{2}\alpha_s^2}{4G_F V_{tb}V_{ts}^* m_{\tilde{q}}^2}(\delta^d_{LL})_{23}\left[-\frac{7}{3}B_1(x) + \frac{1}{3}B_2(x) + \frac{1}{6}P_1(x) + \frac{3}{2}P_2(x)\right] \ , \\
C_5^{\tilde{g}}(M_S) &\simeq \frac{\sqrt{2}\alpha_s^2}{4G_F V_{tb}V_{ts}^* m_{\tilde{q}}^2}(\delta^d_{LL})_{23}\left[\frac{10}{9}B_1(x) + \frac{1}{18}B_2(x) - \frac{1}{18}P_1(x) - \frac{1}{2}P_2(x)\right] \ , \\
C_6^{\tilde{g}}(M_S) &\simeq \frac{\sqrt{2}\alpha_s^2}{4G_F V_{tb}V_{ts}^* m_{\tilde{q}}^2}(\delta^d_{LL})_{23}\left[-\frac{2}{3}B_1(x) + \frac{7}{6}B_2(x) + \frac{1}{6}P_1(x) + \frac{3}{2}P_2(x)\right] \ , \\
C_{7\gamma}^{\tilde{g}}(M_S) &\simeq -\frac{\sqrt{2}\alpha_s\pi}{6G_F V_{tb}V_{ts}^* m_{\tilde{q}}^2}\left[(\delta^d_{LL})_{23}\left(\frac{8}{3}M_3(x) - \mu_H \tan\beta \frac{m_{\tilde{g}}}{m_{\tilde{q}}^2}\frac{8}{3}M_a(x)\right)\right. \\
&\qquad \left. +(\delta^d_{LR})_{23}\,\frac{m_{\tilde{g}}}{m_b}\,\frac{8}{3}M_1(x)\right] \ , \\
C_{8G}^{\tilde{g}}(M_S) &\simeq -\frac{\sqrt{2}\alpha_s\pi}{2G_F V_{tb}V_{ts}^* m_{\tilde{q}}^2}\left[(\delta^d_{LL})_{23}\left\{\left(\frac{1}{3}M_3(x) + 3M_4(x)\right)\right.\right. \\
&\qquad \left.\left. -\mu_H \tan\beta \frac{m_{\tilde{g}}}{m_{\tilde{q}}^2}\left(\frac{1}{3}M_a(x) + 3M_b(x)\right)\right\} + \ (\delta^d_{LR})_{23}\,\frac{m_{\tilde{g}}}{m_b}\left(\frac{1}{3}M_1(x) + 3M_2(x)\right)\right] \ .
\end{aligned} \tag{4}$$

Here $B_{1,2}$, $P_{1,2}$, M_{1-4} and $M_{a,b}$ are the loop functions[3] and $x = m_{\tilde{g}}^2/m_{\tilde{q}}^2$, where $m_{\tilde{g}}$ is the gluino mass. The superscript $\tilde{g}$ denotes the coefficients come from the gluino contributions. The other contributions include those from the SM, the charged Higgs, the chargino and the neutralino. We note that these contributions except for gluino one have no extra CP violating phases once we consider the experimental constraint from the electron, neutron and atomic EDMs. Consequently, the CP violating and flavor changing phenomena are generally less sensitive to these operators and controlled by the gluino contributions.

The penguin coefficients $C_{3-6}^{\tilde{g}}$ depend only on $(\delta^d_{LL})_{23}$, on the other hand the dipole-penguin coefficients $C_{7\gamma}^{\tilde{g}}$ and $C_{8G}^{\tilde{g}}$ on both $(\delta^d_{LL})_{23}$ and $(\delta^d_{LR})_{23}$. In particular that of the $(\delta^d_{LL})_{23}$ contributions to $C_{7\gamma}^{\tilde{g}}$ and $C_{8G}^{\tilde{g}}$ are enhanced by a ratio of the Higgs VEVs, $\tan\beta$, because of the double-mass-insertion diagrams. This type of diagrams is composed of $(\delta^d_{LL})_{23}$ and $(\delta^d_{LR})_{33}$. We note the diagram is very similar to one of $(\delta^d_{LR})_{23}$. To see this argument more clearly, let

[3]The loop functions $B_{1,2}$, $P_{1,2}$ and M_{1-4} are defined in Ref. [11]. M_a and M_b are the same as M_1 and M_2 in Ref. [3], respectively.

us denote the Wilson coefficients as

$$C_{7\gamma}^{\tilde{g}} \propto \left[(\delta_{LL}^d)_{23} + c^{7\gamma}(\delta_{LR}^d)_{23}\right], \quad C_{8G}^{\tilde{g}} \propto \left[(\delta_{LL}^d)_{23} + c^{8G}(\delta_{LR}^d)_{23}\right], \tag{5}$$

and define "total mixing",

$$(\delta_{LL}^d)_{23}^{(\mathrm{tot})} \equiv (\delta_{LL}^d)_{23} + c^{7\gamma,8G}(\delta_{LR}^d)_{23}. \tag{6}$$

Here the coefficient c's are estimated as $c \simeq (\delta_{LR}^d)_{33}^{-1}$ up to the loop functions. It is important that c's satisfy $c^{8G}/c^{7\gamma} (\simeq \tilde{c}^{8G}/\tilde{c}^{7\gamma}) \simeq 1$ within an error about 40 %. If this relation is exact, the result from the contribution with $(\delta_{LL}^d)_{23}$ become the same as that with $(\delta_{LR}^d)_{23}$ in the processes dominated by $C_{7\gamma}^{\tilde{g}}$ and $C_{8G}^{\tilde{g}}$. That is, we can study $(\delta_{LL}^d)_{23}$ and $(\delta_{LR}^d)_{23}$ simultaneously, and $(\delta_{RR}^d)_{23}$ and $(\delta_{RL}^d)_{23}$, too. In this letter we first investigate the LL and RR squark mixings and then discuss to distinguish LR and RL from them.

Let us review the processes which we consider in this letter. The $b \to s$ effective Hamiltonian induces a lot of FCNC processes. The important observables in this letter are the following CP violating ones: $S_{\phi K_S}$, $S_{\eta' K_S}$, $S_{K^*\gamma}$ and $A_{\mathrm{CP}}^{b\to s\gamma}$. The supersymmetry contributions can be comparable to or even larger than that of the SM, and depend dominantly on the dipole moment operators, $C_{7\gamma}$ and C_{8G}. We determine the the imaginary part of the "total" squark mixings by these processes.

The $B_s - \overline{B_s}$ mixing, ΔM_s, is also interesting here. ΔM_s depends on the four-quark operators and the double-mass-insertion diagrams do not dominate. As a result, it is possible to distinguish the LL and RR mixings from the others by this process. As will be mentioned later only a product of $(\delta_{LL}^d)_{23}$ and $(\delta_{RR}^d)_{23}$ induces large ΔM_s [13], which may be detected at LHC [14, 15].

Too large MIA parameters however exceed the current bounds from $\mathrm{Br}(b \to s\gamma)$ and the contribution of the strange quark color electric-dipole-moment operator (CEDM) to the neutron and atomic EDMs. We consider these processes as a constraint on the parameter space.

We comment on the model parameters in this letter. Here the $b \to s$ transition processes are selected so that a number of the parameters is as small as possible. In fact, the relevant soft parameters are the squark masses $m_{\tilde{q}}$, the gluino mass $m_{\tilde{g}}$, the higgsino mass parameter μ_H and $\tan\beta$ (and top trilinear coupling for the contribution to the strange CEDM from chargino mediated diagram [2]). Also the real part of the Wilson coefficients includes the neutralino and chargino masses and the charged Higgs mass.

Before proceeding to each modes, we comment on the other FCNC processes. There are attractive observables other than those in this letter. For example, $B_s \to l\,l$ is triggered by mediating the Higgses and may become sizable [16]. However the supersymmetry contributions to the observables depend strongly on additional model parameters like Higgs mass ones. Thus we do not consider those processes in this letter.

The branching ratio of the inclusive decay $b \to s\gamma$ is one of the most important processes when we consider the $b \to s$ transition. In fact the branching ratio is proportional to the sum of the squared Wilson coefficients, $(|C_{7\gamma}(m_b)|^2 + |\widetilde{C}_{7\gamma}(m_b)|^2)$, at the leading order. And the SM prediction of the branching ratio, which can be calculated cleanly, is now in agreement with experimental data [17] within errors. In consequence, too large $b \to s$ transition amplitude is excluded by considering $\mathrm{Br}(b \to s\gamma)$ [18]. The theoretical prediction has been calculated at next-to-leading order in renormalization group improved perturbation theory and its error is about 10 % [19]. It is expected to be reduced down to 5 % within a few years when all next-to-next-to-leading-order corrections are included [19]. The experimental error will be also reduced 10 % to 5 % at super B factory after one year of running [20]. Despite of these expectations, we consider $\mathrm{Br}(b \to s\gamma)$ just as a constraint on the parameter space and are less interested in detection ability of supersymmetry in this letter. Thus we take a rather conservative value,

$$2.0 \times 10^{-4} < \mathrm{Br}(b \to s\gamma) < 4.5 \times 10^{-4}, \tag{7}$$

instead of improved value which we expect in the near future.

The MIA parameters are also constrained by the EDMs, though there are large hadronic uncertainties left. The squark mixings contribute to the strange quark CEDM and the CEDM is limited by the neutron and atomic EDMs. The neutron EDM now gives the strongest bound [3],

$$e|\tilde{d}_s| < 1.9(2.4) \times 10^{-25}\ e\mathrm{cm}, \tag{8}$$

where the number in the parentheses represents the assumption of the Pecci-Quinn (PQ) symmetry. The measurement of the deuteron EDM is also proposed and its sensitivity is $\sim 10^{-26}\ e$cm. As a result, at first we find that the gluino diagram contributions generically impose strong correlations on the squark mixings [1, 3],

$$\begin{aligned} \sqrt{|\mathrm{Im}(\delta^d_{LL})_{23}(\delta^d_{RR})_{32}|} &\lesssim 1.6(2.0) \times 10^{-4}, \\ \sqrt{|\mathrm{Im}(\delta^d_{LL})_{23}(\delta^d_{LR})_{32}|} \quad \text{and} \quad \sqrt{|\mathrm{Im}(\delta^d_{LR})_{23}(\delta^d_{RR})_{32}|} &\lesssim 4.4(5.6) \times 10^{-6}, \end{aligned} \tag{9}$$

for the soft masses $m_{\tilde{g}} = m_{\tilde{q}} = 500$ GeV and $\mu_H \tan\beta = 5000$ GeV. In this letter we thus assume that the phases of the squark mixings are perfectly aligned. Finally the chargino diagram also gives a sizable contribution to the strange CEDM [2]. The contribution leads to a constraint on the LL squark mixings, $|\mathrm{Im}(\delta^d_{LL})_{23}| \lesssim 10^{-1}$, in the generic situation. It is comparable to $\mathrm{Br}(b \to s\gamma)$, and detailed analysis shows that it is rather parameter dependent [8].

$B_d \to \phi K_S$ and $B_d \to \eta' K_S$ are very interesting decay modes in the search for new physics [1, 6–8]. In the SM the both mixing-induced CP asymmetries for ϕK_S and $\eta' K_S$ are

equal to $\sin(2\phi_1)$, which is measured by a tree dominated process $B_d \to J/\Psi K_S$. Any deviation larger than $\mathcal{O}(\lambda^2)$ would be a signal for new physics [21]. The mixing-induced CP asymmetry for a CP eigenstate $f_{\rm CP}$ is given by

$$S_{f_{\rm CP}} \;=\; \xi_{f_{\rm CP}} \frac{2\,{\rm Im}\left[e^{-2i\,\phi_1} A(\overline{B_d} \to f_{\rm CP})/A(B_d \to f_{\rm CP})\right]}{|A(\overline{B_d} \to f_{\rm CP})/A(B_d \to f_{\rm CP})|^2 + 1} \;, \tag{10}$$

with ${\rm CP}|f_{\rm CP}\rangle = \xi_{f_{\rm CP}}|f_{\rm CP}\rangle$. New CP violating phases drive the mixing-induced CP asymmetry away from the SM prediction. In the supersymmetry models the deviation is induced by the additional phases of the squark mixings. The dominant supersymmetric contribution comes from the chromo-magnetic penguin, which depends on the squark mixings, and thus induce the deviation of the mixing-induced CP asymmetry. The supersymmetric contribution to the amplitudes in ϕK_S is denoted as,

$$A^{\rm SUSY}(\overline{B_d} \to \phi K_S) \;\propto\; C_{8G}^{\tilde{g}}(m_b) \;+\; \widetilde{C}_{8G}^{\tilde{g}}(m_b) \;. \tag{11}$$

In the case of $\eta' K_S$ it comes from the chromo-magnetic penguin as that of ϕK_S, however the chirality structure is different:

$$A^{\rm SUSY}(\overline{B_d} \to \eta' K_S) \;\propto\; C_{8G}^{\tilde{g}}(m_b) \;-\; \widetilde{C}_{8G}^{\tilde{g}}(m_b) \;, \tag{12}$$

because of parity difference between ϕ and η' [7]. Consequently, we can classify the chromo-magnetic penguin operators, in particular whether $\widetilde{C}_{8G}$ is large or not by using the both data of $S_{\phi K_S}$ and $S_{\eta' K_S}$. The current results are $S_{\eta' K_S} = 0.02 \pm 0.34 \pm 0.03$ at BABAR [22] and $0.43 \pm 0.27 \pm 0.05$ at Belle [4]. Although $S_{\eta' K_S}$ is slightly smaller than the SM prospect, the deviation from $S_{\phi K_S}$ is not yet measured. The experimental errors in $S_{\phi K_S}$ and $S_{\eta' K_S}$ will be less than 0.1 at super B factory so that the discrepancy may be observed in future.

Although the experimental signal is clean, theoretical estimation includes large uncertainties. They originate in the calculations of hadronic matrix elements. To obtain the matrix elements, there are several approaches, naive factorization [23], generalized factorization [24], QCD factorization [25], perturbative QCD [26], and so on. Each method is however plagued with large theoretical uncertainties and it is expected that the estimation will be improved and they will be reduced in future. As a reference, let us use the generalized factorization method. Then the main theoretical error comes from the matrix element of the chromo-magnetic penguin,

$$\langle \phi K_S | O_{8G} | \overline{B_d} \rangle \;=\; -\frac{\alpha_s(m_b)}{4\pi}\,\frac{m_b}{\sqrt{q^2}} \left\langle \phi K_S \left| O_4 + O_6 - \frac{1}{3}(O_3 + O_5) \right| \overline{B_d} \right\rangle \;, \tag{13}$$

where q^2 is the momentum transferred by the gluon in O_{8G}. Though the parameter q^2 is ambiguous in the generalized factorization, this is not an inherent uncertainty in the estimation

of $S_{\phi K_S}$. In fact this can be removed once we apply QCD factorization [25] or perturbative QCD [27]. Rather the method in this letter has an advantageous of simplicity in the analysis. Here we take $q^2 = (M_B^2 - M_\phi^2/2 + M_K^2)/2$ [24]. This argument is also applied for the analysis of $\eta' K_S$ by replacing ϕ with η'.

$S_{K^*\gamma}$ is one of the important observables for the measurement of the squark mixings in $\widetilde{C}_{7\gamma}$. We measure the asymmetry of B_d decay into a CP eigenstate $K^{*0}\gamma(\to K_S\pi^0\gamma)$ [28]. The leading contribution in $B_d \to K^*\gamma$ is the photo-magnetic penguin. Other contributions, which come from O_2 and O_{8G}, are sub-leading [29, 30] and neglected in the following study for simplicity. In consequence, $S_{K^*\gamma}$ is generated from the interference between $C_{7\gamma}$ and $\widetilde{C}_{7\gamma}$ terms:

$$S_{K^*\gamma} \;=\; \frac{2\,\mathrm{Im}\left[e^{-2i\,\phi_1}\widetilde{C}_{7\gamma}(m_b)/C_{7\gamma}(m_b)\right]}{\left|\widetilde{C}_{7\gamma}(m_b)/C_{7\gamma}(m_b)\right|^2 + 1}\,. \tag{14}$$

$S_{K^*\gamma}$ vanishes in the SM since it is suppressed by $2m_s/m_b$ [28]. However if there is a sizable parameter insertion in $\widetilde{C}_{7\gamma}$, the deviation of $S_{K^*\gamma}$ can be large in the MSSM. At the leading level theoretical uncertainty cancels out in the ratio, because the matrix elements for $O_{7\gamma}$ is the same as that for $\widetilde{O}_{7\gamma}$. This is an advantage of $S_{K^*\gamma}$ compared with $S_{\phi K_S}$ and $S_{\eta' K_S}$. The current data is $S_{K^*\gamma} = 0.25 \pm 0.63 \pm 0.14$ at BABAR [31], which is still ambiguous. The error will be reduced to about 0.1 at super B factory [20].

The direct CP asymmetry for $b \to s\gamma$ is sensitive to the LL and LR mixings. This is estimated at the leading order as

$$\begin{aligned} A_{\mathrm{CP}}^{b\to s\gamma} \;=\; & \frac{1}{|C_{7\gamma}(m_b)|^2 + |\widetilde{C}_{7\gamma}(m_b)|^2}\Big[a_{27}\,\mathrm{Im}\left(C_2(m_b)C_{7\gamma}^*(m_b) + \widetilde{C}_2(m_b)\widetilde{C}_{7\gamma}^*(m_b)\right) \\ & + a_{28}\,\mathrm{Im}\left(C_2(m_b)C_{8G}^*(m_b) + \widetilde{C}_2(m_b)\widetilde{C}_{8G}^*(m_b)\right) \\ & + a_{87}\,\mathrm{Im}\left(C_{8G}(m_b)C_{7\gamma}^*(m_b) + \widetilde{C}_{8G}(m_b)\widetilde{C}_{7\gamma}^*(m_b)\right)\Big]\,, \end{aligned} \tag{15}$$

with $a_{27} \sim \mathcal{O}(10^{-2})$, $a_{28} \sim \mathcal{O}(10^{-3})$ and $a_{87} \sim \mathcal{O}(10^{-1})$ [32]. Although the analysis at the next-to-leading order is given in Ref. [19], we use the result at the leading level for simplicity. The direct CP asymmetry requires at least two amplitudes with different weak phases and different strong phases. In the SM, there is no relative weak phase between $C_{7\gamma}$ and C_{8G} while C_2 has a different one. Consequently, the SM prediction due to the interference between C_2 and $C_{7\gamma}$ is estimated as $\mathcal{O}(10^{-1})$ % [19]. On the other hand, $\widetilde{C}_2$, $\widetilde{C}_{7\gamma}$ and $\widetilde{C}_{8G}$ are suppressed sufficiently in the SM. The current experimental data, $0.025 \pm 0.050 \pm 0.015$ at BABAR [33] and $0.002 \pm 0.050 \pm 0.030$ at Belle [34], are consistent with null asymmetry. Their errors will be reduced to less than 1 % at super B factory [20]. If there is a sizable contribution from the squark mixings on $C_{7\gamma}$ and C_{8G}, the interference between them can generate larger CP

asymmetry, at most 10 %, considering that a_{87} is much larger than the others. However the supersymmetry contributions to $\widetilde{C}_2$, $\widetilde{C}_{7\gamma}$ and $\widetilde{C}_{8G}$ except for that from the gluino diagrams are again negligible. As a result, though the gluino contribution may be sizable, the phase of $\widetilde{C}_{7\gamma}$ aligns with that of $\widetilde{C}_{8G}$ and the CP asymmetry induced by $\widetilde{C}$ sector is still small.

The $B_s - \overline{B_s}$ mixing is helpful to distinguish the mass insertions scheme, that is, a product of the LL and RR mixings, LL+RR, and the others. The gluino contributions to the mass difference between the mass eigenstates of the $B_s - \overline{B_s}$ system is given by

$$\begin{aligned}\frac{\Delta M_s^{\tilde{g}}}{\Delta M_s^{\rm SM}} &= a_1\left[(\delta^d_{LL})^2_{23} + (\delta^d_{RR})^2_{23}\right] + a_2\left[(\delta^d_{LR})^2_{23} + (\delta^d_{RL})^2_{23}\right] \\ &\quad + a_3\left[(\delta^d_{LR})_{23}(\delta^d_{RL})_{23}\right] + a_4\left[(\delta^d_{LL})_{23}(\delta^d_{RR})_{23}\right] , \end{aligned} \tag{16}$$

with $a_1 \sim 1.44$, $a_2 \sim 27.57$, $a_3 \sim -44.76$ and $a_4 \sim -175.79$ for the soft masses $m_{\tilde{g}} = m_{\tilde{q}} = 500$ GeV [13]. The sizable LL+RR contribution enhances ΔM_s significantly but the others do not. So far there has been only the lower bound, $\Delta M_s > 14.5\,\mathrm{ps}^{-1}$ [35]. On the other hand, the SM prediction is typically around $18\,\mathrm{ps}^{-1}$ [36] where its theoretical uncertainty coming from hadronic parameters is about 10 % in the lattice calculations [37]. In the near future, ΔM_s will be measured at Tevatron and/or LHC. LHC covers ΔM_s range up to $48\,\mathrm{ps}^{-1}$ and 95 % exclusion region up to $58\,\mathrm{ps}^{-1}$ after one year of running [14]. And expected statistical uncertainty on ΔM_s is $0.018\,\mathrm{ps}^{-1}$ at $\Delta M_s = 50\,\mathrm{ps}^{-1}$ [15].

By considering the observables, $S_{\phi K_S}$, $S_{\eta' K_S}$, $S_{K^*\gamma}$, $A_{\rm CP}^{b\to s\gamma}$ and ΔM_s, we study potential to constrain and measure the imaginary part of the squark mixings. Here let us summarize the setup in this analysis. At first we consider the situation that a large anomaly in $S_{\phi K_S}$ will be measured at super B factory. Actually such a large deviation is currently implied by the Belle result. In order to realize large deviation in $S_{\phi K_S}$ the MIA parameters are favored to have the maximal phase by considering the constraint from $\mathrm{Br}(b \to s\gamma)$ and the hadronic EDMs. Therefore we assume the squark mixings to be pure imaginary in the following analysis.

Secondly we study the measurement ability for the squark mixings at super B factory. This means that we do not consider the uncertainties due to the calculation method of the $b \to s$ processes. For example, although we use the generalized factorization method for estimating $S_{\phi K_S}$, the technique is expected to be improved in future and the uncertainties may be reduced. In addition, other than the squark mixings we have other relevant model parameters. Those parameters are assumed to be measured at LHC and we do not include their ambiguities in the result. We consider only experimental errors as the resultant uncertainties.

Third, some processes in this letter are planned to be measured at LHC and super B factory. We consider an era after one year of running at super B factory. Currently the proposed luminosity is not settled yet and the expected experimental errors for each processes at super KEKB are summarized in Table. 1 [20]. With these values the squark mixings are determined and we show the result for the both cases of the luminosities.

Fourth, the experimental uncertainty of ΔM_s is proposed to be negligibly small at LHC. As a result, the theoretical uncertainty becomes much larger than the experimental error, unlike the other observables in this letter. Thus we consider the theoretical ambiguity for ΔM_s. We use a value 10 % for the uncertainty in the following.

Let us show the numerical result based on the setup given above. At first we assume the LR and RL squark mixings to be zero. Therefore the total mixings satisfy with $(\delta^d_{LL,RR})^{(\mathrm{tot})}_{23} = (\delta^d_{LL,RR})_{23}$. Figure 1 displays the numerical estimation of $S_{\phi K_S}$, $S_{\eta' K_S}$, $S_{K^*\gamma}$ and $A_{\mathrm{CP}}^{b\to s\gamma}$. We show the constant contours of these observables for changing the squark mixings, $(\delta^d_{LL})_{23}$ and $(\delta^d_{RR})_{23}$. Here we take the other model parameters as, the relevant soft masses (including μ_H) $m_{\mathrm{soft}} = 500$ GeV and $\tan\beta = 10$. Some parameter regions are excluded experimentally. The region of larger $(\delta^d_{LL})_{23}$ and/or $(\delta^d_{RR})_{23}$ exceeds the bound from $\mathrm{Br}(b \to s\gamma)$. Also too large $(\delta^d_{LL})_{23}$ suffers from the EDMs. Here we show the bound from the neutron EDM with the PQ symmetry, though this constraint is weaker for this parameter set.

In Fig. 1 we take a center value of each mode as $S_{\phi K_S} = 0.3$, $S_{\eta' K_S} = 0.5$, $S_{K^*\gamma} = -0.3$ and $A_{\mathrm{CP}}^{b\to s\gamma} = 0.02$. Although these are just reference, we choose $S_{\phi K_S}$ to have a large deviation from the SM considering the current result from Belle. Each experimental uncertainty is denoted as the band at the luminosity of 5 ab^{-1} for Fig. 1 (a) and 50 ab^{-1} for (b), except for $A_{\mathrm{CP}}^{b\to s\gamma}$. Indeed a signal of $A_{\mathrm{CP}}^{b\to s\gamma}$ may be measured at super B factory as long as $\mathrm{Im}(\delta^d_{LL})_{23}$ is large, the parameters here is not suitable to determine the squark mixings from $A_{\mathrm{CP}}^{b\to s\gamma}$, because of the wide extent of the uncertainty. Actually, we note the edge of the $A_{\mathrm{CP}}^{b\to s\gamma}$ error band is drawn in Fig. 1. In addition, we take $\Delta M_s = 50$ ps^{-1} with 10 % error as explained above.

The squark mixings are determined by $S_{\phi K_S}$, $S_{\eta' K_S}$ and $S_{K^*\gamma}$. As noted above since their dependences to the squark mixings are different, the MIA parameters can be measured. There is a region where the uncertainty band of all these observables overlaps with each other, which is filled by yellow and enclosed by red solid lines in the figures. From Fig. 1 we find that for the luminosity 5 ab^{-1} the squark mixings are determined with an error of $20 - 40$ %, on the other hand, the result is improved when the luminosity is 50 ab^{-1} and its uncertainty becomes about 10 %.

FCNC is also induced by the LR and RL mixings. We consider these mixings as an origin of flavor mixings instead of the LL and RR case. Since we focus on the dipole-penguin dominant processes, as stressed above the contours of these processes are found to be nearly the same as the LL and RR ones except for the scale of the axes, which are approximately rescaled by c's in Eq. (6). Actually the contour lines in Fig. 1 just shift about 30 % at most for the rescaled axes. As a result the error estimation of the resultant squark mixings becomes the same as that of LL and RR, and we obtain the uncertainties of $20 - 40$ % for 5 ab^{-1} and about 10 % for 50 ab^{-1}.

The mixture case of the LL, RR, LR and RL squark mixings is more complex. When

the contributions from these four mixings are comparable, the uncertainty width is larger than the result estimated above. This is because the coefficients c's do not satisfy with $c^{8G}/c^{7\gamma}(= \tilde{c}^{8G}/\tilde{c}^{7\gamma}) = 1$ exactly. Therefore, if we have no information on the ratios of the squark mixings, the error bands become about 30 % wider. In that case, the total mixings are consequently determined with the uncertainties about 40 % at the luminosity of 50 ab^{-1}.

In order to identify the four squark mixings, the $B_s - \overline{B_s}$ mixing is useful because ΔM_s is controlled by the product of the LL and RR squark mixings. Figure 2 shows the constant contours of ΔM_s for varying the ratio of LR (RL) component. On the other hand, in this figure the total mixings $(\delta^d_{LL,RR})^{(\mathrm{tot})}_{23}$ are fixed and as a result the other observables in the Fig. 1 change little. Hence from ΔM_s we obtain one relation for the squark mixings in the fixed total mixings.

In particular, we can definitely distinguish the LL+RR case from the others by observing large ΔM_s. Furthermore when both the LL and RR mixings are dominant, ΔM_s is helpful to measure those mixings more precisely. In fact from Fig. 1 the error band is very narrow even when we consider the theoretical uncertainty. This is striking when we measure the squark mixings at the lower luminosity of 5 ab^{-1}. On the other hand, the mixture case is more complex and we need detailed analysis.

In the above discussion we assumed the condition that the phase of all squark mixings align to each other. One of the reasons comes from the experimental constraint from the EDMs. Although the LL (LR) squark mixing is forced to align with RR (RL), when both the RR and RL mixings are very suppressed the relative phase between LL and LR mixings becomes loose. And the exchanged case of $L \leftrightarrow R$ is also true. Then the phase may induce larger uncertainty in the squark mixings. However even in such a special case, since we are interested in the situation that anomaly of $S_{\phi K_S}$ is large here, the phase is favored to be maximal. Consequently, we reproduce the above result.

A different choice of center values of the observables modifies the result. The error band of $S_{K^*\gamma}$ becomes wide in contrast to $S_{\phi K_S}$ and $S_{\eta' K_S}$ when $(\delta^d_{RR})^{(\mathrm{tot})}_{23}$ increases. Furthermore we will not expect sizable $A_{\mathrm{CP}}^{b\to s\gamma}$ there. As a result, in such a region the total RR squark mixing may be measured with larger uncertainty, though the total LL squark mixing is again determined at the same level in Fig. 1.

We comment on the dependence of the result to the other model parameters and the effects from the real part of the squark mixings. First let us consider other sets of the soft masses. When the gluino, the scalar bottom and the scalar strange become heavy, all the $b \to s$ transition amplitudes are suppressed and vice versa. As a result, the uncertainties of the squark mixings change little. On the other hand, the chargino contributions to the hadronic EDMs have different dependence to the soft masses. They are enhanced by smaller up-type squark and chargino masses, contrary to the other observables and constraint. In such

a case, the LL squark mixing is bounded strongly and the uncertainty becomes large. Also the higgsino mass parameter enhances the gluino contributions to the observables, but do not the chargino contributions too much. Therefore the region of smaller μ_H may again suffer from the hadronic EDMs. We note that the LR mixing is however free from the constraint. Second, other choices of the masses of the chargino, the neutralino and the charged Higgs modify the real part of the Wilson coefficients. However the effect is weak and we obtain the almost same result. Finally, the future measurement of $S_{\phi K_S}$ may inform us that the squark mixings are not restricted to be pure imaginary. Then the non-vanishing real part generally makes the uncertainties large. In such a case, we need more information on the model parameters by some additional observables.

Finally we touch on the flavor-changing neutral Higgs boson decays into the bottom and strange quarks. In the SM, the W boson exchange diagram contributes to the mode, and the result is found to be very small. On the other hand, the gluino exchange diagram with the squark mixing generally induces a flavor-changing coupling of the Higgs. The authors in Ref. [38] showed that the supersymmetry contribution can overshoot that of the SM. In fact it becomes larger by about three orders of magnitude when the squark mixing takes the value used in the above analysis. Then such a large branching ratio of the flavor-changing Higgs decay may be detected at LHC.

When LHC starts running and confirms supersymmetry, we come to the next stage, that is, to determine the parameters in supersymmetry models and to investigate physics at higher energy. Super B factory is very appropriate to measure the squark mixings, which induce FCNC and CP violation. In this letter we studied potential to constrain and measure the squark mixings at super B factory. With the prospected data after one year of running we found the mixings is determined at about 10 % level at best. However this result is based on theoretical improvements of estimation and on some assumptions. Thus we need more rigorous studies.

Acknowledgment

M.E. thanks the Japan Society for the Promotion of Science for financial support. The work of S.M. was supported in part by the Grants-in-aid from the Ministry of Education, Culture, Sports, Science and Technology, Japan, No.14046201.

References

[1] J. Hisano and Y. Shimizu, Phys. Lett. B **581**, 224 (2004).

[2] M. Endo, M. Kakizaki and M. Yamaguchi, Phys. Lett. B **583**, 186 (2004).

[3] J. Hisano and Y. Shimizu, arXiv:hep-ph/0406091.

[4] K. Abe *et al.* [Belle Collaboration], Phys. Rev. Lett. **91** (2003) 261602.

[5] B. Aubert *et al.* [BABAR Collaboration], arXiv:hep-ex/0403026.

[6] T. Moroi, Phys. Lett. B **493**, 366 (2000); E. Lunghi and D. Wyler, Phys. Lett. B **521**, 320 (2001); D. Chang, A. Masiero and H. Murayama, Phys. Rev. D **67**, 075013 (2003); S. Khalil and E. Kou, Phys. Rev. D **67**, 055009 (2003); G. L. Kane, P. Ko, H. b. Wang, C. Kolda, J. H. Park and L. T. Wang, arXiv:hep-ph/0212092; Phys. Rev. Lett. **90**, 141803 (2003); R. Harnik, D. T. Larson, H. Murayama and A. Pierce, Phys. Rev. D **69**, 094024 (2004); M. Ciuchini, E. Franco, A. Masiero and L. Silvestrini, Phys. Rev. D **67**, 075016 (2003) [Erratum-ibid. D **68**, 079901 (2003)]; S. Baek, Phys. Rev. D **67**, 096004 (2003); R. Arnowitt, B. Dutta and B. Hu, Phys. Rev. D **68**, 075008 (2003); M. Ciuchini, A. Masiero, L. Silvestrini, S. K. Vempati and O. Vives, Phys. Rev. Lett. **92** (2004) 071801; S. Mishima and A. I. Sanda, Phys. Rev. D **69**, 054005 (2004); J. F. Cheng, C. S. Huang and X. H. Wu, arXiv:hep-ph/0404055; E. Gabrielli, K. Huitu and S. Khalil, arXiv:hep-ph/0407291; G. L. Kane, H. Wang, L. T. Wang and T. T. Wang, arXiv:hep-ph/0407351.

[7] S. Khalil and E. Kou, Phys. Rev. Lett. **91**, 241602 (2003).

[8] M. Endo, M. Kakizaki and M. Yamaguchi, arXiv:hep-ph/0403260.

[9] T. Goto, Y. Okada, Y. Shimizu, T. Shindou and M. Tanaka, arXiv:hep-ph/0306093.

[10] L. J. Hall, V. A. Kostelecky and S. Raby, Nucl. Phys. B **267**, 415 (1986).

[11] F. Gabbiani, E. Gabrielli, A. Masiero and L. Silvestrini, Nucl. Phys. B **477**, 321 (1996).

[12] G. Buchalla, A. J. Buras and M. E. Lautenbacher, Rev. Mod. Phys. **68**, 1125 (1996).

[13] P. Ball, S. Khalil and E. Kou, Phys. Rev. D **69**, 115011 (2004).

[14] P. Ball *et al.*, arXiv:hep-ph/0003238.

[15] The LHCb Collaboration, *LHCb Technical Proposal*, CERN/LHCC/98-4.

[16] K. S. Babu and C. F. Kolda, Phys. Rev. Lett. **84**, 228 (2000).

[17] R. Barate *et al.* [ALEPH Collaboration], Phys. Lett. B **429** (1998) 169; S. Chen *et al.* [CLEO Collaboration], Phys. Rev. Lett. **87** (2001) 251807; K. Abe *et al.* [Belle Collaboration], Phys. Lett. B **511** (2001) 151; P. Koppenburg *et al.* [Belle Collaboration], arXiv:hep-ex/0403004; B. Aubert *et al.* [BABAR Collaboration], arXiv:hep-ex/0207074; B. Aubert *et al.* [BABAR Collaboration], arXiv:hep-ex/0207076; C. Jessop, SLAC-PUB-9610.

[18] A. L. Kagan and M. Neubert, Eur. Phys. J. C **7**, 5 (1999).

[19] T. Hurth, E. Lunghi and W. Porod, arXiv:hep-ph/0312260.

[20] A. G. Akeroyd *et al.*, arXiv:hep-ex/0406071.

[21] Y. Grossman and M. P. Worah, Phys. Lett. B **395**, 241 (1997); arXiv:hep-ph/9707280; D. London and A. Soni, Phys. Lett. B **407**, 61 (1997); Y. Grossman, G. Isidori and M. P. Worah, Phys. Rev. D **58**, 057504 (1998).

[22] B. Aubert *et al.* [BABAR Collaboration], Phys. Rev. Lett. **91**, 161801 (2003).

[23] M. Wirbel, B. Stech and M. Bauer, Z. Phys. C **29**, 637 (1985).

[24] A. Ali and C. Greub, Phys. Rev. D **57**, 2996 (1998); A. Ali, G. Kramer and C. D. Lu, Phys. Rev. D **58**, 094009 (1998).

[25] M. Beneke, G. Buchalla, M. Neubert and C. T. Sachrajda, Phys. Rev. Lett. **83**, 1914 (1999); Nucl. Phys. B **591**, 313 (2000).

[26] Y. Y. Keum, H. n. Li and A. I. Sanda, Phys. Lett. B **504**, 6 (2001); Phys. Rev. D **63**, 054008 (2001).

[27] S. Mishima and A. I. Sanda, Prog. Theor. Phys. **110**, 549 (2003)

[28] D. Atwood, M. Gronau and A. Soni, Phys. Rev. Lett. **79**, 185 (1997).

[29] S. W. Bosch and G. Buchalla, Nucl. Phys. B **621**, 459 (2002).

[30] Y. Y. Keum, M. Matsumori and A. I. Sanda, arXiv:hep-ph/0406055.

[31] B. Aubert *et al.* [BABAR Collaboration], arXiv:hep-ex/0405082.

[32] A. L. Kagan and M. Neubert, Phys. Rev. D **58**, 094012 (1998).

[33] B. Aubert *et al.* [BABAR Collaboration], Phys. Rev. Lett. **93**, 021804 (2004).

[34] S. Nishida *et al.* [BELLE Collaboration], Phys. Rev. Lett. **93**, 031803 (2004).

[35] The Heavy Flavor Averaging Group, http://www.slac.stanford.edu/xorg/hfag/

[36] M. Battaglia *et al.*, arXiv:hep-ph/0304132.

[37] N. Yamada *et al.* [JLQCD Collaboration], Nucl. Phys. Proc. Suppl. **106**, 397 (2002); D. Becirevic, V. Gimenez, G. Martinelli, M. Papinutto and J. Reyes, **0204**, 025 (2002); S. M. Ryan, Nucl. Phys. Proc. Suppl. **106**, 86 (2002).

[38] S. Bejar, F. Dilme, J. Guasch and J. Sola, arXiv:hep-ph/0402188.

Observable	5 ab^{-1}	50 ab^{-1}
$A_{\rm CP}^{b\to s\gamma}$	0.011	0.005
$S_{K^{*0}\gamma}$	0.14	0.04
$\Delta S_{\phi K_S}$	0.079	0.031
$\Delta S_{\eta' K_S}$	0.049	0.024

Table 1: Experimental errors after one year of running at super KEKB [20].

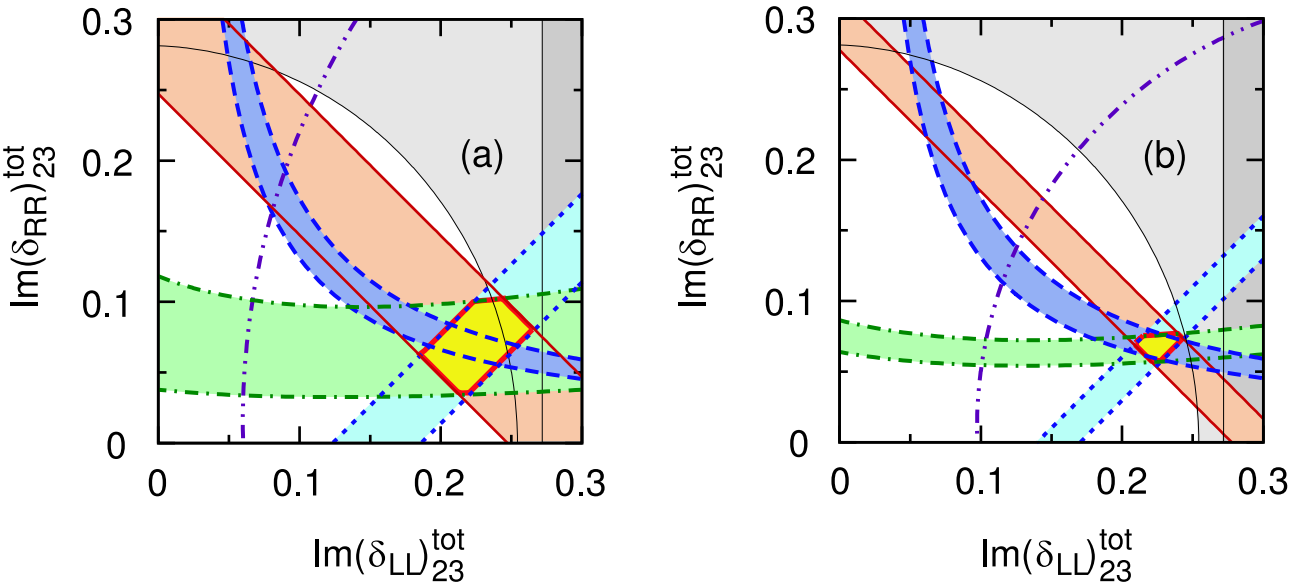

Figure 1: The constant contours of $S_{\phi K_S}$(red or thick solid), $S_{\eta' K_S}$(light blue or dotted), $S_{K^*\gamma}$(green or dash-dotted), $A_{\rm CP}^{b\to s\gamma}$(purple or dash double-dotted) and ΔM_s(blue or dashed) for changing the LL and RR squark mixings. Here we take all soft parameters $m_{\rm soft} = 500$ GeV and $\tan\beta = 10$. The bands of the experimental errors are displayed at the luminosity (a) 5 ab^{-1} and (b) 50 ab^{-1}, except for $A_{\rm CP}^{b\to s\gamma}$. Although $A_{\rm CP}^{b\to s\gamma}$ will be measured at the region of larger $\mathrm{Im}(\delta^d_{LL})^{(\rm tot)}_{23}$, it is ambiguous in this parameter set. We also note that ΔM_s is estimated in the condition that the LL+RR squark mixings are dominant. There is a region where the uncertainty band of $S_{\phi K_S}$, $S_{\eta' K_S}$ and $S_{K^*\gamma}$ overlaps with each other, which is filled by yellow and enclosed by red solid lines in the figures. Some parameter regions are excluded experimentally: the region of larger $(\delta^d_{LL})^{(\rm tot)}_{23}$ and/or $(\delta^d_{RR})^{(\rm tot)}_{23}$, which is outer side of the thin solid lines, comes from $\mathrm{Br}(b\to s\gamma)$(light shadowed) and larger $(\delta^d_{LL})^{(\rm tot)}_{23}$ from the EDMs(dark shadowed).

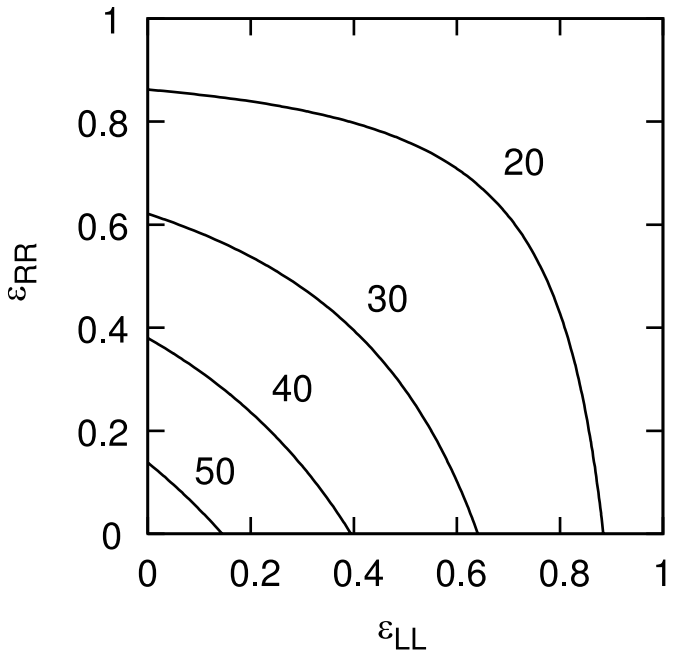

Figure 2: The constant contours of the $B_s - \overline{B_s}$ mixing, ΔM_s. The axes are $\epsilon_{LL} = c^{8G}(\delta^d_{LR})_{23}/(\delta^d_{LL})^{(\mathrm{tot})}_{23}$ and $L \leftrightarrow R$ for ϵ_{RR}. Here $(\delta^d_{LL,RR})^{(\mathrm{tot})}_{23}$ of the chromo-magnetic penguin are fixed.